Excitation function studies of α induced reactions for niobium and preequilibrium effects

Avinash Agarwal,* I. A. Rizvi, and A. K. Chaubey†
Department of Physics, Aligarh Muslim University, Aligarh-202 002, India
(Received 15 February 2001; published 12 February 2002)

Excitation functions of the reaction (α,n), $(\alpha,2n)$, $(\alpha,3n)$, and $(\alpha,\alpha n)$ for ^{93}Nb were measured up to 37 MeV using the stacked foil activation technique and high-purity Ge γ-ray spectroscopy method. The measured experimental values were compared with the geometry-dependent hybrid model in which the emission of particles prior to the equilibrium decay is taken into account whenever the interaction of projectile with the target nucleus is considered. It was found that the compound nucleus decay mechanism alone is unable to explain the experimental trend of our data. The isomeric cross-section ratios (σ_m/σ_g) for the $(\alpha,2n)$ reaction were also calculated as a function of α-particle energy. A definite trend was observed in the variation of the ratio with α-particle energy.

DOI: 10.1103/PhysRevC.65.034605 PACS number(s): 25.55.−e, 27.60.+j

I. INTRODUCTION

The study of the effect of preequilibrium (PE) emission followed by equilibrium (EQ) decay to the excitation function in the multiparticle emission process has been a point of interest for the last several years. The presence of a preequilibrium component in any reaction can be observed from the high-energy tail of the excitation function, which cannot be reproduced by the statistical model. The presence of a preequilibrium reaction can also be inferred from the study of the variation of the isomeric cross-section ratio with energy. Many attempts have been made to understand such reactions. Starting from the pioneering work of Griffin [1], which provides the first explanation of the spectral shape of the excitation function in the framework of exciton model, many other semiclassical models have been proposed [2–6]. The hybrid and geometry-dependent hybrid (GDH) models [5,6] proposed by Blann have been found to be relatively simple and closed-form models for the successful reproduction of the experimental data. Apart from these semiclassical models of the nuclear reaction for the successful reproduction of the excitation function data, efforts are in progress to give a full quantum-mechanical picture in the framework of multistep theories proposed by Feshbach, Kerman, and Koonin [7] and others [8–10]. For the interaction of a composite particle such as an α particle, the quantum-mechanical picture is yet to come.

For a better understanding of the PE emission mechanism more and more experimental data are necessary. A lot of work has been done on the study of the excitation function of α-particle-induced reactions for various target nuclei [11] over a wide range of energy and over a wide range of the periodic table. However, the situation regarding it is still unsatisfactory, as there are large discrepancies in the reported values even for a single specific reaction. Moreover, the data are incomplete and contain considerable errors. Although the cross sections for niobium were measured earlier by few groups [12–17] using the single γ ray for each reaction, even then their results differ to a large extent; hence precise and accurate measurements are still needed. With this in mind, we have made an attempt to measure the reaction cross section for ^{93}Nb up to 37 MeV α-particle energy using the maximum possible γ rays for a single reaction. As a check, the relative intensities of identified γ rays were also measured. A theoretical analysis of data has also been carried out under the prescription of the GDH model [6].

II. EXPERIMENTAL DETAILS

The excitation functions for the α-induced reactions on ^{93}Nb were measured by the stacked foil activation technique and γ-ray spectroscopy method. The stack was made with spectroscopically pure niobium foils of thickness 10.5 mg/cm^2. The niobium foil was cut into pieces of size 1.5 cm$\times$1.5 cm, and each of them was glued to an aluminum frame, having a circular hole of diameter 1.2 cm in its center. Energy degrader aluminum foils of different thickness were sandwiched between the target foils, so as to get the desired α-particle energy incident on each foil. The stack was irradiated with a 40 MeV diffused beam of diameter 8 mm at the Variable Energy Cyclotron Centre, Calcutta (India). The beam energy was determined from a curve that related the cyclotron rf with energy constructed from experimental data on elastic scattering. The irradiation was performed with a beam current of about 380 nA so that a few hours only of well-controlled irradiation was sufficient to excite the required activities. The α-particle flux was calculated using a Faraday cup and charge integrator. A copper foil of thickness 10.68 mg/cm^2 was also used as a flux monitor for checking the flux, and good agreement was found with less than 10% discrepancy. The experimental setup with details is given elsewhere [18].

The activities induced in the target foils were followed using a high-resolution (2 keV for 1332 keV γ ray of ^{60}Co) high-purity Ge (HPGe) detector of 100 cm^3 active volume coupled to the Ortec's PC-based multichannel analyzer. The dead time for counting was kept less than 10% by adjusting the target detector separation in these measurements, and proper account of the dead time was taken in the calcula-

*Present address: Department of Physics, Bareilly College, Bareilly (U.P.), India.
†Electronic address: pht18akc@amu.up.nic.in

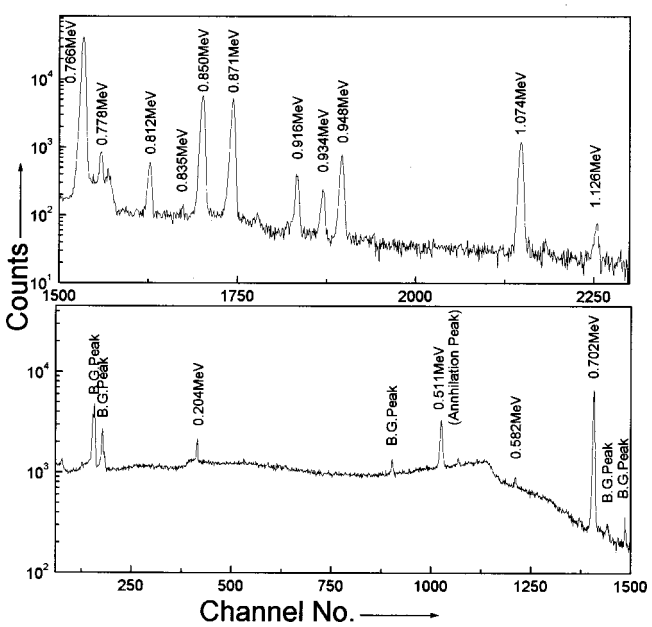

FIG. 1. Typical γ-ray spectrum obtained from the activation of the ^{93}Nb target by 28.6 MeV α particles.

tions. Several spectra were taken at suitable intervals to permit identification of the half-lives of various residual nuclei. A typical γ-ray spectrum obtained from the activation of niobium target foil at 28.6 MeV is shown in Fig. 1.

The energy and efficiency calibration of the HPGe spectrometer was done using various standard sources, i.e., ^{22}Na, ^{57}Co, ^{60}Co, ^{133}Ba, and ^{152}Eu of known strengths. The geometry dependent efficiency (ϵG) of the detector for different source-detector distances was computed using the relation

$$\epsilon G = C e^{\lambda t}/S_0 \theta,$$

where C is the number of counts per second under the photopeak, λ is the decay constant of the radioactive nuclei, t is the time lapse between start of counting and the date of fabrication of standard γ-ray source, S_0 is the actual number of radioactive quanta emitted by the standard source per second at the time of its fabrication, and θ is the absolute intensity of the relevant γ ray. The values of θ and λ were taken from

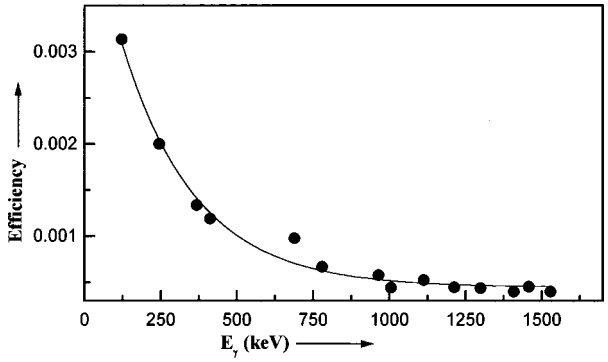

FIG. 2. Geometry-dependent efficiency of the HPGe detector at a source detector distance of 15.5 cm.

TABLE I. Reaction channels for 37 MeV α particles incident on ^{93}Nb.

Reaction	Q value (MeV)	$T_{1/2}$	E_γ (MeV)	Absolute γ intensity (%)
^{93}Nb$(\alpha,n)^{96m}$Tc	−7.01	51.5 min	0.778	1.9
			1.200	1.0
^{93}Nb$(\alpha,n)^{96g}$Tc		4.35 d	0.314	2.4
			0.316	1.4
			0.778	99.1
			0.812	81.5
			0.850	96.9
			1.127	15.1
^{93}Nb$(\alpha,2n)^{95m}$Tc	−14.92	61.0 d	0.204	66.2
			0.582	32.5
			0.786	9.0
			0.821	4.9
			0.835	28.1
			1.039	3.0
^{93}Nb$(\alpha,2n)^{95g}$Tc		20.0 h	0.766	93.0
			0.948	2.1
			1.074	4.2
^{93}Nb$(\alpha,3n)^{94m}$Tc	−24.85	52.5 min	0.871	94.0
			0.993	2.2
^{93}Nb$(\alpha,3n)^{94g}$Tc		4.88 h	0.449	2.6
			0.532	2.6
			0.702	99.8
			0.850	97.7
			0.871	100.0
			0.916	7.4
^{93}Nb$(\alpha,\alpha n)^{92m}$Nb	−8.96	10.14 d	0.913	1.6
			0.934	99.2
^{93}Nb$(\alpha,\alpha n)^{92g}$Nb		3.2×10^7 yr		
^{93}Nb$(\alpha,2p)^{95m}$Nb	−12.59	3.5 d	0.204	2.4
			0.235	25.5
^{93}Nb$(\alpha,2p)^{95g}$Nb		35 d	0.766	99.8

Ref. [19]. The values of ϵG thus obtained were plotted as a function of energy using the program ORIGIN 5.0. A polynomial of degree 4 having the following form was found to give the best fit for these curves:

$$\epsilon G = a_0 + a_1 X + a_2 X^2 + a_3 X^3 + a_4 X^4,$$

where a_0, a_1, a_2, a_3, and a_4 are the coefficients having different values for different source detector distances. X is the energy of the characteristic γ ray. A typical geometry-dependent efficiency curve of the 100 cm^3 HPGe detector obtained at a distance of 15.5 cm from the detector surface is shown in Fig. 2. The following expression was used for computing the experimentally measured reaction cross sections [18]:

$$\sigma(E) = \frac{A\lambda \exp(\lambda t_2)}{N_0 \phi(\epsilon G)\theta K\{1-\exp(-\lambda t_1)\}\{1-\exp(-\lambda t_3)\}},$$

TABLE II. Experimental cross section for (α,n), $(\alpha,2n)$, $(\alpha,3n)$, and $(\alpha,\alpha n)$ reactions.

	Cross section (mb)											
	$(\alpha,n)^{96}$Tc		$(\alpha,2n)^{95g}$Tc		$(\alpha,2n)^{95m}$Tc		$(\alpha,2n)^{95}$Tc		$(\alpha,3n)^{94}$Tc		$(\alpha,\alpha n)^{92g}$Nb	
E_α (MeV)	Present	Previous	Present	Previous	Present	Previous	Present	Previous	Present	Previous	Present	Previous
18.0		786[a]						569[a]				
20.8±1.6		170±21[b]		605±79[b]		90.0±11[b]		695±79.8[b]				
21.1		203[a]						1162[a]				
21.2		276±30[c]		232±28[c]		93.4±13.1[c]		325.4±30.9[c]				3.1±0.5[c]
23.0		92±7[d]		849±66[d]								
23.3±1.3	70.7±0.6		606.9±10.6		80.0±12.3		686.9±16.2		24.2±1.3		4.5±0.7	
24.2±1.4		43±5[b]		943±126[b]		103±13[b]		1046±126.7[b]				5.7±0.8[b]
24.4		106±15[c]		489±54[c]		169±22[c]		658±58.3[c]				14.6±2.8[c]
26.1±1.2	30.0±1.2		714.4±9.1		65.5±12.8		779.9±15.8		18.5±0.9		6.9±0.7	
28.0								1612[a]		86[a]		
28.2±1.4		22.5±2.8[b]		994±133[b]		77±9.8[b]		1071±133.4[b]		56±7.8[b]		11.6±1.6[b]
28.6±1.1	22.5±0.7		684.0±8.8		41.7±12.5		725.7±15.3		57.7±1.1		9.8±0.7	
29.0		22±2.4[d]		913±74[d]						83±6[d]		
29.5		22.6±3.4[c]		665±67[c]		203±24[c]		868±71.2[c]		8.21±1.2[c]		26.4±3.9[c]
30.9±1.0	18.2±0.5		588.6±7.9		70.0±10.3		658.7±12.9		239.7±1.9		11.9±0.7	
31.8±1.2		15.7±2.0[b]		560±74[b]		37±4.7[b]		597±74.2[b]		269±36[b]		14.0±1.9[b]
32.6				666[d]						397[d]		
33.2±0.9	13.7±0.7		394.3±6.9		31.0±10.5		425.2±12.6		449.1±2.2		14.4±0.7	
34.0								620[a]		876[a]		
34.1				387±30[d]						518±40[d]		
34.3		20.5±3.1[c]		812±81[c]		223±27[c]		1035±85.4[c]		119±15[c]		32.3±3.9[c]
35.3±0.9	17.9±0.6		399.9±9.9		24.2±15.7		424.1±18.6		853.2±3.0		18.3±1.0	
36.0±1.2		10.3±1.3[b]		311±41[b]		19±2.5[b]		330±41.1[b]		700±94[b]		15.0±2.0[b]
37.4±0.8	14.3±0.9		295.9±7.2		11.7±7.4		307.6±10.3		1139.3±16.5		14.6±0.9	
38.0		12.8±1.9[c]		349±38[c]		91.8±12.8[c]		440.8±133.5[c]		485±49[c]		39.6±4.7[c]
38.4								263[a]		1060[a]		
38.8				184±15[d]						684±53[d]		
39.8				152[d]						768[d]		
39.8±1.2		8.3±1.0[b]		161±21[b]		12.7±1.7[b]		173.7±21.1[b]		768±103[b]		17.7±2.3[b]
40.0		11.5±0.1[e]		227±3[e]					1023±18.0[e]		18.3±0.5[e]	

[a]Reference [12].
[b]Reference [13].
[c]Reference [15].
[d]Reference [14].
[e]Reference [16].

where A is the counts under the photopeak of the characteristic γ ray, λ is the decay constant of the product nucleus, N_0 is the number of nuclei of the isotope under investigation, ϕ is the incident α-particle flux, ϵG is the geometry-dependent efficiency of the HPGe detector, θ is the absolute intensity of the characteristic γ rays, K is the self-absorption correction factor for the γ ray in the sample, t_1 is the irradiation time, t_2 is the time lapse between stopping the beam and the start of counting, and t_3 is the counting time.

The energy of the α particles striking different target foils has been calculated by taking into account the thickness of the foil and the energy loss within it, using the stopping power table of Northcliffe and Schilling [20]. No consideration of straggling for the increase in the path of the incident beam in the stopping material has been made for the estimation of energy loss in the target thickness because of its negligibly small effects for α particles [14].

III. EXPERIMENTAL RESULTS

In the present work the various reactions induced by α particles on ^{93}Nb were observed by detecting the characteristic γ rays obtained from the decay of residual nuclei. The possible reaction channels for ^{93}Nb (residual nucleus unstable) in the energy range considered in the present measurement are listed in Table I. The other details, viz., residual nucleus, Q value, half-life γ-ray energies, and corresponding absolute intensities, are also given in the table. The Q values of the different reactions have been taken from Ref. [21] and

TABLE III. Isomeric ratios of product nuclides for the $(\alpha,2n)$ reaction.

	Isomeric ratio (σ_m/σ_g)			Isomeric ratio (σ_m/σ_g)	
E_α (MeV)	Present	Previous	E_α (MeV)	Present	Previous
18.0		0.160[a]	29.5		0.094[b]
		0.330[a]	29.9		0.071[a]
18.5		0.169[b]	30.5		0.091[b]
19.0		0.169[b]	30.9±1.0	0.119	
19.7		0.154[a]	31.8		0.062[a]
20.8±1.6		0.109[c]	31.8±1.2		0.061[c]
21.1		0.125[a]	33.0		0.085[b]
		0.137[a]	33.2±0.9	0.078	
21.2		0.402[d]	33.5		0.093[b]
22.0		0.145[b]	34.0		0.062[a]
22.5		0.143[b]			0.064[a]
22.6		0.133[a]			0.085[b]
23.0		0.139[b]	34.3		0.275[d]
23.3±1.3	0.132		34.5		0.099[b]
24.0		0.139[b]	35.0		0.088[b]
24.2±1.4		0.077[c]	35.3±0.9	0.061	
24.4		0.346[d]	35.4		0.056[a]
25.2		0.097[a]	35.5		0.099[b]
25.5		0.123[b]	36.0±1.2		0.061[c]
26.0		0.128[b]	36.5		0.111[b]
26.1±1.2	0.091		37.4±0.8	0.040	
26.5		0.115[b]	38.0		0.263[d]
27.0		0.111[b]			0.122[b]
28.0		0.085[a]	38.4		0.071[a]
		0.230[a]			0.060[a]
		0.104[b]	38.5		0.128[b]
28.2±1.4		0.066[c]	39.8±1.2		0.092[c]
28.6±1.1	0.061		40.0		0.164[b]
29.5		0.305[d]			

[a]Reference [12].
[b]Reference [17].
[c]Reference [13].
[d]Reference [15].

other decay data from Ref. [19]. In the list very weak γ rays are not included whenever strong γ rays are available for the same emitting nuclide. γ rays having higher energies are also not included in the list. We have considered only those γ rays that gave appreciable activities for the meaningful excitation studies. The γ-ray spectroscopy software package RADWARE [22] was used extensively for analyzing the spectrum.

The activation cross section for a given reaction was determined from the intensities of the various γ rays identified as arising from the same residual nucleus. The reported value is the weighted average [23] of the various cross-section values so obtained. The statistical error given in the results is the larger one of the internal and external errors [23]. In general these errors are less than 31% except for few points.

A. (α,n) reaction

This reaction produces two isomers of ^{96}Tc. Both isomers are unstable. The ground state has a half-life of 4.35 d and a metastable state of 51.5 min. The reaction producing the ground-state isomer was studied by considering the 0.778, 0.812, 0.850, and 1.127 MeV γ rays. In the analysis the 0.850 MeV photopeak was not used at energies above the threshold for $(\alpha,3n)$ reaction, as this γ ray is also associated with the $(\alpha,3n)$ reaction. The 0.778 MeV γ ray is common to both isomers. However, this peak can be used in the analysis after the decay of metastable-state activity. The cross sections for this reaction obtained at different energies are tabulated in Table II.

The metastable state of ^{96}Tc decays to the ground state with 98% isomeric transition and 2% electron capture and β^+ decay. The half-life of the metastable state is much shorter than that of the ground state. Therefore, the cross sections for the ground-state-producing reaction as obtained above is almost the total cross section for the production of ^{96}Tc isomers as the activities were measured after the decay of the metastable state.

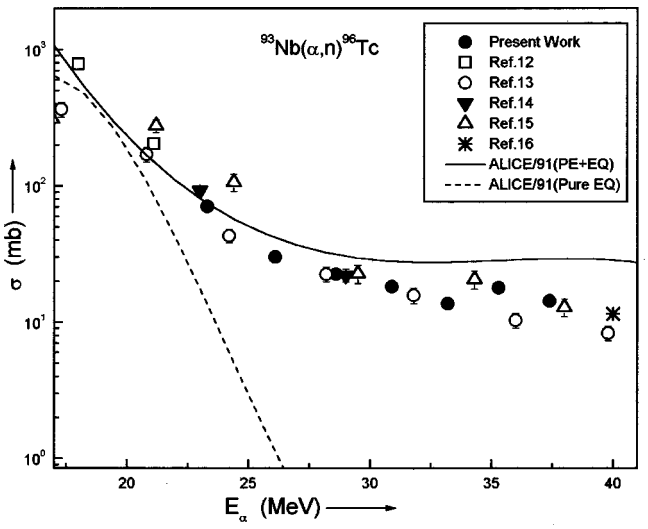

FIG. 3. Experimental and theoretical excitation functions for the ^{93}Nb$(\alpha,n)^{96}$Tc reaction.

B. $(\alpha,2n)$ reaction

The $(\alpha,2n)$ reaction on ^{93}Nb produces two isomers of ^{95}Tc with half-lives of 20.0 h and 61.0 d. The 0.766 MeV γ ray emitted from the ground-state isomer is common with that of the $(\alpha,2p)^{95g}$Nb reaction. Therefore, the cross sections for the $(\alpha,2n)^{95g}$Tc reaction have been measured by considering the 0.948 and 1.074 MeV γ rays. The cross sections obtained for this reaction are given in Table II.

The metastable state of ^{95}Tc decays to the ground state with 95.8% EC, 0.3% β^+ decay, and 3.9% isomeric transition. The main γ rays obtained from its decay are 0.204, 0.582, and 0.835 MeV. The 0.204 MeV γ ray is also emitted from ^{93}Nb$(\alpha,2p)^{95m}$Nb reaction ($Q=-12.6$ MeV) with an absolute intensity of 2.4%. Another γ ray of 0.235 MeV having the absolute intensity of 25.5% is also emitted from the ^{95m}Nb isomer. The counts under the photopeak of 0.204 MeV due to the ^{93}Nb$(\alpha,2p)^{95m}$Nb reaction can be estimated if one can measure the cross section of this reaction by considering the 0.235 MeV photopeak. However, in the present measurements a background photopeak of the same energy

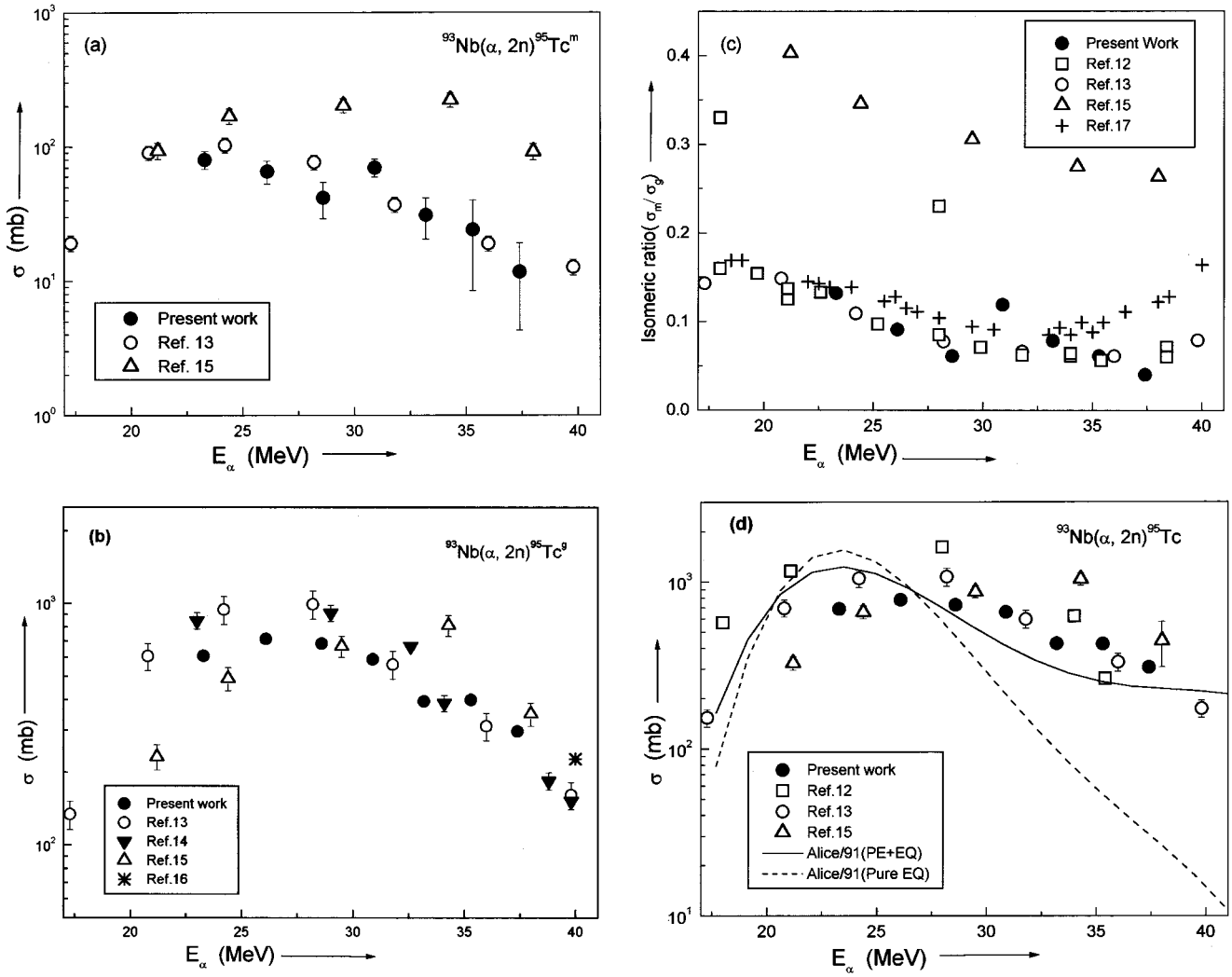

FIG. 4. (a) Experimental excitation function for the ^{93}Nb$(\alpha,2n)^{95m}$Tc reaction. (b) Experimental excitation function for the ^{93}Nb$(\alpha,2n)^{95g}$Tc reaction. (c) Isomeric cross-section ratio (σ_m/σ_g) of the ^{93}Nb$(\alpha,2n)^{95}$Tc reaction as a function of α-particle energy. (d) Experimental and theoretical excitation functions for the ^{93}Nb$(\alpha,2n)^{95}$Tc reaction.

TABLE IV. Measured relative intensities of identified γ rays.

γ-ray energy E_γ (keV)	Absolute abundance θ (%)	Normalized relative intensity: Present measurement	Normalized relative intensity: Literature value[a]
Reaction ^{93}Nb$(\alpha,n)^{96g}$Tc, $t_{1/2}$ of product nucleus 4.35 d			
0.778	99.1	100.0	100.0[b]
0.812	81.5	81.9±3.5	82.2
0.850	96.9	97.9±4.0	97.8
1.127	15.1	14.9±0.8	15.2
Reaction ^{93}Nb$(\alpha,2n)^{95m}$Tc, $t_{1/2}$ of product nucleus of 61.0 d			
0.204	66.2	100.0	100.0[b]
0.582	32.5	49.0±7.1	49.1
0.835	28.1	43.9±2.0	42.5
Reaction ^{93}Nb$(\alpha,2n)^{95g}$Tc, $t_{1/2}$ of product nucleus 20.0 h			
0.766	93.0	100.0	100.0[b]
0.948	2.1	2.2±0.1	2.3
1.074	4.2	4.5±0.2	4.5
Reaction ^{93}Nb$(\alpha,3n)^{94g}$Tc, $t_{1/2}$ of product nucleus 4.88 h			
0.702	99.8	93.2±4.0	99.8[b]
0.871	100.0	100.0	100.0
0.916	7.4	7.2±0.3	7.4
Reaction ^{93}Nb$(\alpha,\alpha n)^{92m}$Nb, $t_{1/2}$ of product nucleus 10.14 d			
0.934	99.2		100.0

[a]Reference [19].

[b]Normalization has been done with respect to this value from literature.

was obtained; hence the cross section for the ^{93}Nb$(\alpha,2n)^{95m}$Tc was studied considering the 0.582 and 0.835 MeV γ rays only. The cross sections for this reaction are presented in Table II, and the isomeric cross-section ratios (σ_m/σ_g) are shown in Table III.

C. $(\alpha,3n)$ reaction

Two isomers of ^{94}Tc are produced in this reaction. The ground and metastable states have half-lives of 4.88 h and 52.5 min, respectively. The ground-state isomer has four major γ rays, viz., 0.702, 0.850, 0.871, and 0.916 MeV. The 0.850 MeV γ ray is common with ^{96g}Tc, produced in the (α,n) reaction, whereas the 0.871 MeV γ ray is also obtained from the ^{94m}Tc. The 0.871 MeV γ ray has also been used in the analysis of the ground-state-producing reaction by counting the activities after several half-lives of the metastable state. Thus, the cross sections of the $(\alpha,3n)^{94g}$Tc reaction have been measured considering the 0.702 and 0.916 MeV γ rays. The cross sections obtained for this reaction are tabulated in Table II.

D. $(\alpha,\alpha n)$ reaction

This reaction produces two isomers of ^{92}Nb with half-lives of 3.2×10^7 yr and 10.14 d, the latter being the metastable state. The same residual nuclei are also produced by the $(\alpha,2p3n)$ reaction. The Q value for this reaction is -37.1 MeV. Below the threshold for the $(\alpha,2p3n)$ reaction (i.e., 38.7 MeV) the experimental cross sections are solely for the $(\alpha,\alpha n)$ reaction. The ground-state activity is negligible because of its long half-life. The metastable state has an intense γ ray of 0.934 MeV. The cross section for $(\alpha,\alpha n)^{92m}$Nb reaction has been measured using the 0.934 MeV γ ray and is shown in Table II.

IV. MODEL CALCULATIONS

The excitation functions of the α-particle-induced reaction on ^{93}Nb were evaluated theoretically using the computer code ALICE/91 [24]. The code ALICE/91 [24] employs the Weisskopf-Ewing model [25] for the statistical component and hybrid model [5] as well as geometry-dependent hybrid model of Blann [6] for the pre-equilibrium emission. The statistical part of ALICE/91 [24] can account for a large variety of reaction types. Besides evaporation of neutrons and protons (according to Weisskopf and Ewing [25]), clusters such as deuterons and α particles can be considered. This is done with conservation of angular momentum. The binding energies and Q values used in the present code are based on experimental masses (Wapastra and Audi [26]). The ALICE/91 code stores experimental masses in the data file. Whenever the nuclear masses are not available in the data file they are calculated from the Myers-Swiatecki mass formula [27] (liquid drop mass with pairing). The pairing energy δ is calculated from the backshifted model. In these calculations the pairing energy is zero for even-even nuclides, $-\delta$ for odd-even nuclides, and -2δ for odd-odd nuclides, with $\delta=11/\sqrt{A}$. The inverse cross sections are calculated from the optical model subroutine, which uses the Becchetti and Greenless [28] optical parameters. The intranuclear transition rates are calculated using the Pauli-corrected nucleon-nucleon (N-N) scattering cross sections, and adjustment of the mean free path intranuclear transitions is done by keeping the so-called mean free path multiplier (k) constant equal to 3.0.

Level densities of residual nuclei play an important role in deciding the shapes and absolute value of the excitation functions. For calculations, the level density formula proposed by Lang and Le Couteur [29] was used. In general, for the level density parameter a value of $a=A/K$ was applied, where A denotes the nucleon number and K a constant the values of which spread over a wide region and have been given in the literature [30,31]. In our calculations, a best fit was obtained by using a value of 8.0.

In preequilibrium reactions, the initial exciton configuration is a crucial quantity. The influence of this initial exciton configuration on the result of PE calculations was investigated by varying the initial exciton configuration $n_0(n\text{-}p\text{-}h)$, which is described by the number of neutrons (n) and protons (p) in excited states and the number of holes (h) after the first collision. The total exciton n_0 equals the sum of n, p, and h. For α-induced reactions, the initial exciton number $n_0=4$ or 5 was suggested by Blann [3]. However, it was found by many investigators [32–35] that $n_0=4$ fits experimental data better than $n_0=5$. We have performed the calculations with an initial exciton configuration $n_0=4$ $(2n+2p+0h$, i.e., a pure particle state).

A physical interpretation of an initial exciton configura-

tion $n_0=4$ $(2n+2p+0h)$ is that only four excitons initially share an excitation energy, which is equivalent to a breakup of the incoming α particle in the field of nucleus and nucleons occupying the excited states above a completely filled Fermi sea.

V. RESULTS AND DISCUSSION

The measured relative intensities of identified γ rays are tabulated in Table IV. It can be seen from Table IV that the currently measured relative intensities are in good agreement with their respective literature values [19]. Our experimentally measured values along with earlier measurements [12–17] are shown in Figs. 3–6. The vertical bars represent the total estimated errors in the cross sections. If no bar is depicted, the size of the circle includes the magnitude of the statistical errors. The experimental excitation functions were also compared with those predicted by theory, on the basis of compound and precompound reaction mechanisms. Comparison with theory is made only for those reactions in which the total cross section (i.e., both isomers *m* and *g*) was measured in the present work. The excitation functions are represented by the solid line for the cross section obtained by the consideration of both the compound and precompound contributions (GDH model calculation) and by the dashed line for the compound nucleus (Weisskopf-Ewing calculation) cross sections.

The excitation functions for the (α,n) reaction are shown in Fig. 3. The results of other workers [12–16] are also included in the figure. It is seen from the figure that the various experimental results vary within a factor of 2.5 at about 24.4 MeV. It is also seen that the excitation function cannot be reproduced by the compound nucleus theory in the high-energy region. It is reproduced well by taking into account the precompound contribution.

The excitation functions for the $(\alpha,2n)$ reaction are shown in Figs. 4(a) and 4(b) for the metastable and ground states, respectively. In these figures results of other workers [13–16] are also included. The results of Mukharjee, Rashid, and Chintalapudi [15] are exceptionally higher for the $(\alpha,2n)^{95m}$Tc reaction while lower in the $(\alpha,2n)^{95g}$Tc reaction (up to 24.4 MeV) from our results as well as other reported values. The isomeric cross-section ratio (σ_m/σ_g) for the $(\alpha,2n)$ reaction with the other reported results [12,13,15,17] as a function of α-particle energy is shown in Fig. 4(c). One of the exceptions is the result of Branquinho *et al.* [12] at 18 and 28 MeV, where the authors repeated the measurements and observed a variation of the ratios within a factor of 2.5 at the same energy. Again the results of Mukharjee, Rashid, and Chintalapudi [15] are exceptionally high in the whole energy range. The overall cross-section ratios indicate that the population of the ground state (spin $\frac{9}{2}^+$) is more probable than that of the isomeric state (spin $\frac{1}{2}^-$) in the present energy region. The decrease in ratio with increasing energy is due to the fact that probabilities of populating the higher spin states increases with energy as higher angular momenta are imparted at higher energies. The total cross section for the $(\alpha,2n)$ reaction as a function of α-particle energy is shown in Fig. 4(d). Results of other workers [12,13,15] are also included in this figure. It can be seen from Fig. 4(d) that the results of Branquinho *et al.* [12] are high (up to 34.0 MeV). The results of Mukharjee, Rashid, and Chintalapudi [15] are lower than our results up to 24.4 MeV. It is also seen that the excitation functions can be represented by compound nucleus theory up to 27 MeV. Above this energy, a better fit to the experimental data could be obtained by taking the pre-equilibrium contribution into consideration.

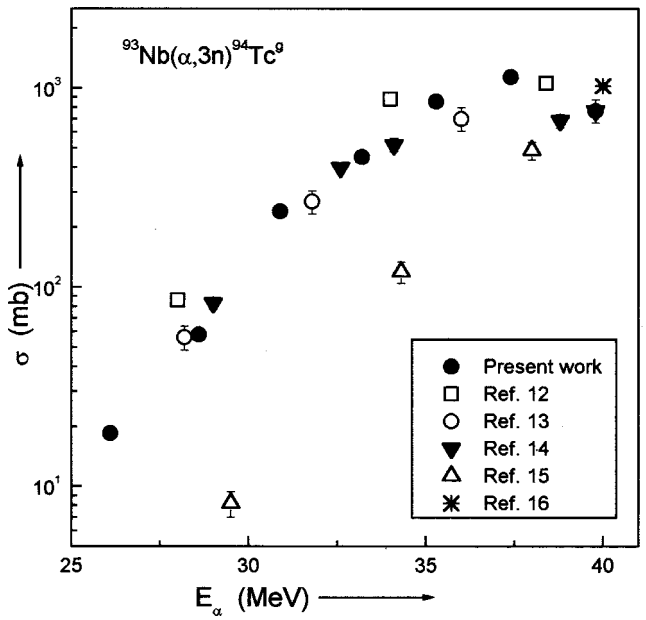

FIG. 5. Experimental excitation function for the ^{93}Nb$(\alpha,3n)^{94g}$Tc reaction.

The cross sections for the $(\alpha,3n)$ reaction were measured only for the ground-state-producing reaction and are shown in Fig. 5. Results of other workers [12–16] are also included in this figure. It can be seen from this figure that our results agree with those of Singh, Agarwal, and Rao [13] and Ernst *et al.* [14]. The cross sections reported by Branquinho *et al.* [12] are higher than our results, while results of Mukharjee, Rashid, and Chintalapudi [15] are lower. Since we measured only the ground-state cross sections it is not appropriate to compare our results with theory.

Cross sections for the $(\alpha,\alpha n)$ reaction were measured only for the reaction leading to the metastable state of ^{92}Nb. It is shown in Fig. 6 together with other reported results [13,15,16]. Our results agree with those of Singh, Agarwal, and Rao [13] in the whole energy region, while the results of Mukharjee, Rashid, and Chintalapudi [15] are higher than our results and also with the results of Singh, Agarwal, and Rao [13]. Comparison of the results with theory is not appropriate since we could not measure the ground-state cross sections. However, we can have some idea of the nuclear reaction mechanism from the theoretical and experimental excitation functions. The theoretical curves show a peak while the experimental peak shows a plateau in the excitation functions. The slow variation in the cross sections suggests that this reaction takes place through the direct reaction mechanism, where the incoming α particle knocks out a neu-

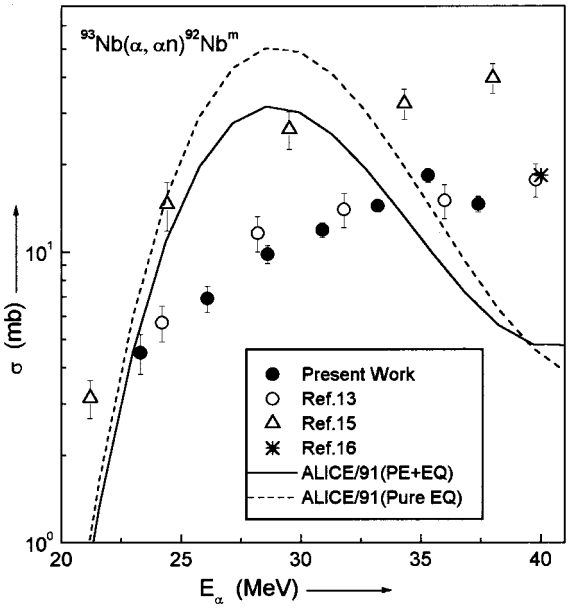

FIG. 6. Experimental and theoretical excitation functions for the ^{93}Nb$(\alpha,\alpha n)^{92}$Nb reaction.

tron from the ^{93}Nb target nucleus, leaving the residual nucleus in an excited state.

VI. CONCLUSIONS

Excitation functions for the (α,n), $(\alpha,2n)$, $(\alpha,3n)$, and $(\alpha,\alpha n)$ reactions on the target element niobium were measured in the present work using the maximum possible γ rays for the single reaction. As a check, the relative intensities of identified γ rays were also measured.

In general, it is quite evident from Figs. 3 and 4(d) that PE emission of multiparticles is necessary before the system is equilibrated and hence the experimentally observed high-energy tail of the excitation functions be explained only when the contribution of semiclassically treated PE emission (GDH model) followed by particle evaporation from the equilibrated system (Weisskopf-Ewing model) is taken into account. The precompound reaction mechanism in its decay is unable to explain the experimental data in the high-energy tail portion of the excitation functions. It is clear from Figs. 3 and 4(d) that the calculated values shown by dashed lines (based on pure equilibrium model) do not reproduce the experimental data well; they are reproduced well only when the preequilibrium emission is also taken into account, as shown by solid lines. The preequilibrium fraction (f_{PE}) [33] of the total reaction cross section has also been calculated at different α-particle energies, which is shown in Fig. 7. It was found that f_{PE} increases with particle energy.

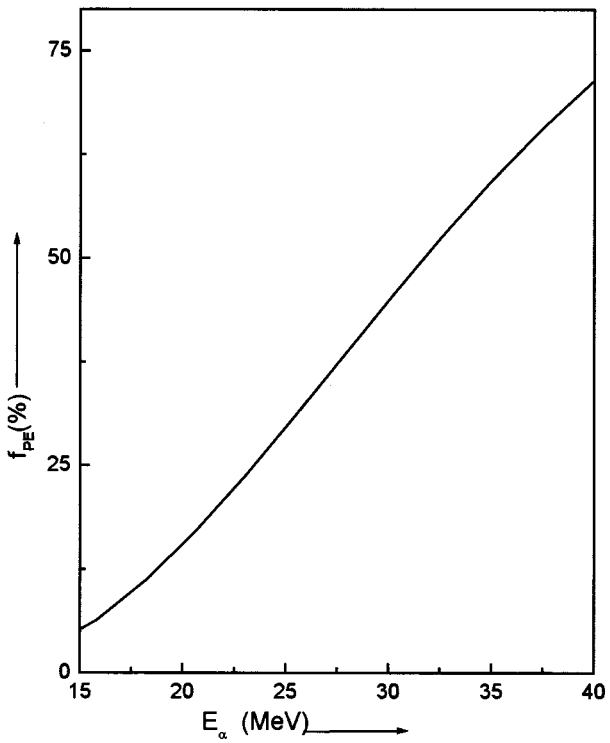

FIG. 7. Preequilibrium fraction $[f_{\mathrm{PE}}(\%)]$ of the total reaction cross section as a function of α-particle energy.

ACKNOWLEDGMENTS

The authors are thankful to the Chairman, Department of Physics, Aligarh Muslim University, Aligarh (India) for providing the necessary facilities to carry out this work. Thanks are also due to Inter University Consortium for DAE facilities Calcutta Centre (India) for financial support through IUC project. In addition, the athors are grateful to Dr. Sandeep Ghugre for discussions.

[1] J. J. Griffin, Phys. Rev. Lett. **17**, 478 (1966).
[2] G. D. Harp and J. M. Miller, Phys. Rev. C **3**, 1847 (1971).
[3] M. Blann, Ann. Nucl. Sci. **25**, 123 (1975).
[4] E. Gadioli, E. Gadioli-Erba, and P. G. Sona, Nucl. Phys. **A217**, 589 (1973).
[5] M. Blann, Phys. Rev. Lett. **27**, 337 (1971); **27**, 700(E) (1971); **27**, 1550(E) (1971).
[6] M. Blann, Phys. Rev. Lett. **28**, 757 (1972).
[7] H. Feshbach, A. Kerman, and S. Koonin, Ann. Phys. (N.Y.) **125**, 429 (1980).
[8] L. Avaladi, R. Bonetti, and L. Colli-Milazzo, Phys. Lett. **94B**, 463 (1980).
[9] G. M. Field, R. Bonetti, and P. E. Hodgson, J. Phys. G **12**, 93 (1986).
[10] P. E. Hodgson, International Center for Theoretical Physics Report No. SMR/284-5, 1988.
[11] EXFOR Library, Nuclear Data Section, IAEA, Vienna, 1992.
[12] C. L. Branquinho, S. M. A. Hoffmann, G. W. A. Newton, V. J. Robinson, H. Y. Wang, and I. S. Grant, J. Inorg. Nucl. Chem. **41**, 617 (1979).

[13] N. L. Singh, S. Agarwal, and J. Rama Rao, J. Phys. Soc. Jpn. **59**, 3916 (1990).
[14] J. Ernst, R. Ibowski, H. Klampfl, H. Machner, T. Mayer-Kuckuk, and R. Schnaz, Z. Phys. A **308**, 301 (1982).
[15] S. Mukharjee, M. H. Rashid, and S. N. Chintalapudi, Pramana, J. Phys. **41**, 329 (1993).
[16] E. Gadioli, E. Gadioli-Erba, J. J. Hogan, and B. V. Jack, Phys. Rev. C **29**, 76 (1984).
[17] T. Matsuo, J. M. Matuzek, Jr., N. D. Dudey, and T. T. Sugihara, Phys. Rev. B **39**, 886 (1965).
[18] I. A. Rizvi, M. K. Bhardwaj, M. Afzal Ansari, and A. K. Chaubey, Appl. Radiat. Isot. **41**, 215 (1990).
[19] C. M. Lederer and V. S. Shirley, *Table of Isotopes*, 7th ed. (Wiley, New York, 1978).
[20] L. C. Northcliffe and R. F. Schilling, Nucl. Data, Sect. A **7**, 256 (1970).
[21] A. H. Wapstra and K. Bos, At. Data Nucl. Data Tables **19**, 177 (1977).
[22] D. C. Redford, Nucl. Instrum. Methods Phys. Res. A **371**, 297 (1995).
[23] S. F. Mughabghab, M. Divadeenam, and N. E. Holden, *Neutron Cross Sections* (Academic, New York, 1989), Vol. 1, Part A, p. 89.
[24] M. Blann, ALICE/91, LLNL/IAEA/NEA Data Bank France, 1991.
[25] V. F. Weisskopf and D. H. Ewing, Phys. Rev. **57**, 472 (1942).
[26] A. H. Wapstra and G. Audi, Nucl. Phys. **A432**, 1 (1985).
[27] W. D. Myers and W. J. Swiatecki, Nucl. Phys. **81**, 1 (1966); Ark. Fys. **36**, 343 (1967).
[28] F. D. Becchetti and G. W. Greenless, Phys. Rev. **182**, 190 (1969).
[29] J. M. Lang and K. J. Le Couteur, Proc. Phys. Soc., London, Sect. A **67**, 586 (1954).
[30] G. Horwitz, S. J. Spesser, R. A. Esterland, B. D. Pate, and J. B. Reynolds, Nucl. Phys. **54**, 64 (1964).
[31] D. G. Sarantities, Nucl. Phys. **A93**, 576 (1976).
[32] M. Blann and T. T. Komoto, Phys. Rev. C **29**, 1678 (1984).
[33] M. K. Bhardwaj, I. A. Rizvi, and A. K. Chaubey, Phys. Rev. C **45**, 2338 (1992).
[34] S. Mukharjee, B. Bindu Kumar, M. H. Rashid, and S. N. Chintalapudi, Phys. Rev. C **55**, 255 (1997).
[35] N. L. Singh, M. S. Gadkari, and S. N. Chintalapudi, Phys. Scr. **61**, 550 (2000).